Exact travelling wave solutions for a generalized nonlinear Schrödinger equation

1996 J. Phys. A: Math. Gen. 29 7687

(http://iopscience.iop.org/0305-4470/29/23/027)

J. Phys. A: Math. Gen. **29** (1996) 7687–7703. Printed in the UK

Exact travelling wave solutions for a generalized nonlinear Schrödinger equation

K Hizanidis†, D J Frantzeskakis‡ and C Polymilis‡

† Department of Electrical and Computer Engineering, National Technical University of Athens, 157 73, Athens, Greece

‡ Department of Physics, University of Athens, Panepistimiopolis, 157 84 Athens, Greece

Received 12 January 1996, in final form 29 April 1996

Abstract. A wide class of exact travelling wave solutions of a generalized nonlinear Schrödinger equation (GNLS) is obtained and analysed in detail. This class of solutions incorporates bright and dark solitary waves, periodic waves, unbounded waves and other solitary waves as asymptotic limits of the periodic or unbounded modes. The method of analysis adopted is based on reducing the GNLS to an ordinary differential equation and studying the phase plane of the resulting dynamical system. Application of the obtained results to the problem of propagation of femtosecond duration pulses in nonlinear optical fibres is also discussed.

1. Introduction

The present paper deals with a generalized nonlinear Schrödinger (GNLS) equation of the following form:

$$\mathrm{i}\frac{\partial q}{\partial x} - \frac{s}{2}\frac{\partial^2 q}{\partial t^2} + q|q|^2 - \mathrm{i}\alpha\frac{\partial^3 q}{\partial t^3} + \mathrm{i}\beta\frac{\partial}{\partial t}(q|q|^2) + \mathrm{i}\gamma q\frac{\partial}{\partial t}(|q|^2) = 0. \tag{1}$$

This equation, as well as certain versions of it, have garnered significant interest recently [1–10]. This interest arises mainly from the fact that equation (1) has important applications in nonlinear optics, where it has been used to describe femtosecond pulse propagation in nonlinear optical fibres [5–10]. In this case, q is the normalized complex field envelope, x and t are the normalized coordinate and time, respectively, while the parameter s is the sign of the group velocity dispersion (GVD) [$s = -1(+1)$ for negative or anomalous (positive or normal) GVD]. The coefficients α, β and γ appearing in the GNLS are real constants describing the third-order linear dispersion, the nonlinear dispersion and the retardation effect on the nonlinear part of the refractive index, respectively [5–8]. Notice that in the case $\alpha = \beta = \gamma = 0$ the GNLS is reduced to the conventional form of the nonlinear Schrödinger (NLS) equation, which is completely integrable by means of the inverse scattering transform (IST) [11]. However, in general, equation (1) is not IST integrable, although it can be transformed, under certain conditions, into an IST integrable system, such as the complex modified Korteweg–deVries equation [2, 3], the higher-order NLS equation [6, 8] or the derivative NLS equation [9].

The purpose of the present work is the presentation of a wide class of exact travelling wave solutions of the GNLS, equation (1). The method of analysis adopted is based on reducing equation (1) to an ordinary differential equation (ODE). This is done by using the travelling-mode type of solution with nonlinear shifts to the carrier frequency, wave number

0305-4470/96/237687+17$19.50

and group velocity. Then, the complete study of the phase plane of the dynamical system, whose evolution the ODE in hand describes, is performed. This so-called phase plane analysis [12] leads to the determination of sets of initial conditions, each of which correspond to a certain type of wave solution. In this way, both the conditions of existence and the solutions themselves, including solitary waves (bright and dark), periodic waves, unbounded solutions and other solitary modes as asymptotic limits of the periodic or unbounded modes, are obtained and analysed in detail.

The present paper is organized as follows. In section 2 the GNLS is reduced to a one-dimensional dynamical system, its stability analysis is performed and the shifts to the frequency, wave number and group velocity are derived. Section 3 is devoted to the presentation of both the conditions of existence and the exact travelling wave solutions of the GNLS themselves. A detailed analysis of the integrable Hamiltonian system in hand is given in section 4, together with several important additional features of the various types of derived solutions. Finally, the main conclusions, both of general and special interest, are presented in section 5.

2. Reduction of the GNLS to a one-dimensional dynamical system

In order to derive the travelling wave solutions of equation (1), we consider the gauge transformation

$$q(x,t) = F(\sigma) f(x,t) \tag{2}$$

where

$$f(x,t) = \exp[\mathrm{i}(\kappa x - \Omega t - \theta_0)] \tag{3}$$

and

$$\sigma = t - \Lambda x - \sigma_0. \tag{4}$$

In equations (2)–(4), $F(\sigma)$ is the unknown envelope function assumed (without loss of generality) to be real, θ_0 and σ_0 are the initial values of the carrier and envelope phases, respectively, while the arbitrary real parameters κ, Ω and Λ have to be determined. The parameters κ and Ω are related to the shifts of the original wave number k and frequency ω, respectively, while the parameter Λ^{-1} is the group velocity of the wave in the x–t reference frame and is connected with the shift of the original group velocity v_g (see, for example, [1, 4, 8, 10]).

Upon substituting now the expressions (2)–(4) into equation (1), the real and imaginary parts of the resulting equation, respectively, read

$$(\tfrac{s}{2} + 3\alpha\Omega)F'' + (\kappa - \tfrac{s}{2}\Omega^2 - \alpha\Omega^3)F - (1 + \beta\Omega)F^3 = 0 \tag{5}$$

$$\alpha F''' + (\Lambda - s\Omega - 3\alpha\Omega^2)F' - (3\beta + 2\gamma)F^2F' = 0 \tag{6}$$

where the notation $F' = \mathrm{d}F/\mathrm{d}\sigma$, $F'' = \mathrm{d}^2F/\mathrm{d}\sigma^2$ and $F''' = \mathrm{d}^3F/\mathrm{d}\sigma^3$ has been used. Then, by differentiating equation (5) once, it can be readily seen that the system of equations (5) and (6) is consistent (i.e. the system is not overdetermined) if the following conditions hold:

$$\frac{\kappa - \frac{s}{2}\Omega^2 - \alpha\Omega^3}{\frac{s}{2} + 3\alpha\Omega} = \frac{1}{\alpha}(\Lambda - s\Omega - 3\alpha\Omega^2) = \lambda \tag{7}$$

$$-\frac{3(1 + \beta\Omega)}{\frac{s}{2} + 3\alpha\Omega} = -\frac{1}{\alpha}(3\beta + 2\gamma) = \mu \tag{8}$$

where λ and μ are non-zero constants. Equations (7) and (8) can be solved recursively and the unknown parameters κ, Ω and Λ can be expressed in terms of the coefficients of the GNLS and the constant λ as follows:

$$\Omega = \frac{6\alpha - s(3\beta + 2\gamma)}{12\alpha(\beta + \gamma)} \tag{9}$$

$$\kappa = \tfrac{s}{2}\lambda + 3\lambda\alpha\Omega + \tfrac{s}{2}\Omega^2 + \alpha\Omega^3 \tag{10}$$

$$\Lambda = \lambda\alpha + s\Omega + 3\alpha\Omega^2. \tag{11}$$

As can be seen, equation (9) determines the parameter Ω, which is constant and depends on the coefficients α, β and γ of the GNLS and the sign s of the GVD. At the same time, equation (10) can be seen as a dispersion relation relating the shifts Ω and κ, depending on the value of the constant λ. Finally, equation (11) determines the envelope (group) velocity in the x–t reference frame as a function of the coefficients α, β, γ and the constant λ.

Returning now to the system of equations (5)–(6), it can be readily seen that it is equivalent to the following equation:

$$F'' + \lambda F + \mu F^3 = 0. \tag{12}$$

Equation (12) can be seen as an 'equation of motion' of a one-dimensional dynamical system. Indeed, by multiplying equation (12) by F' and integrating once, we obtain, as constant of integration, the corresponding Hamiltonian function of the aforementioned dynamical system. This function has the following form:

$$H(q, p) = \frac{p^2}{2} + \lambda\frac{q^2}{2} + \mu\frac{q^4}{4} = h \tag{13}$$

where the value of h can be obtained from the initial conditions q_0 and p_0. The conjugate variables q and p correspond to the generalized coordinate $q = F$ and momentum $p = F'$, respectively. Note that for $\lambda = -1$ and $\mu = +1$, equation (13) is the Hamiltonian function of the typical unforced and undamped Duffing oscillator (see, for example, [13]). It is worth noting that once a pair of initial conditions $(q_0, p_0) \equiv (F_0, F_0')$ is chosen (i.e. amplitude and its respective rate of change), the value of h is readily obtained from equation (13). This value remains constant as the corresponding solution obtained from equation (12) evolves in the σ reference frame. Each constant value of h connects the behaviour of the envelope function $q = F$ with its rate of change with respect to the travelling wave coordinate. In general, different values of h correspond to different schemes of evolution, that is, to different behaviour of the envelope functions. Consequently, the set of initial conditions is directly connected with the behaviour of the envelope functions through the corresponding values of h. The investigation of the dynamical behaviour of the envelope functions in the context of equation (12) will yield the correspondence among classes of travelling wave solutions of the GNLS equation (1) and respective sets of initial conditions.

The Hamiltonian, equation (13), represents an integrable system and its dynamical behaviour is investigated by considering the quantities λ, μ and h as parameters. Following the well known stability analysis (as far as the mechanical analogue of the ODE in hand is concerned), we distinguish the following four cases.

Case 1: $\lambda < 0$, $\mu > 0$. There exist three fixed points, namely two elliptic (stable) placed at $[q = \pm(-\lambda/\mu)^{1/2}, p = 0]$, for $h = -\lambda^2/4\mu$ elliptic (stable) and one hyperbolic (unstable) placed at $[q = 0, p = 0]$, for $h = 0$.

Case 2: $\lambda > 0$, $\mu < 0$. In this case there also exist three fixed points, namely one elliptic (stable) placed at $[q = 0, p = 0]$, for $h = 0$ and two hyperbolic (unstable) placed at $[q = \pm(-\lambda/\mu)^{1/2}, p = 0]$, for $h = -\lambda^2/4\mu$.

Case 3: $\lambda < 0$, $\mu < 0$. Only one fixed point exists in this case, namely a hyperbolic (unstable) one, placed at $[q = 0, p = 0]$, for $h = 0$.

Case 4: $\lambda > 0$, $\mu > 0$. Only one fixed point exists, an elliptic (stable) one, placed at $[q = 0, p = 0]$, for $h = 0$.

For convenience, the following scale transformations are now introduced:

$$Q = q|\mu/\lambda|^{1/2} \qquad P \equiv \dot{Q} \equiv \mathrm{d}Q/\mathrm{d}\Sigma \qquad \text{and} \qquad H' = H|\mu|/\lambda^2 \tag{14}$$

where Σ is given by $\Sigma = \sigma|\lambda|^{1/2}$. The new Hamiltonian (omitting the prime for the sake of simplicity) is

$$H(Q, P) = \frac{p^2}{2} + \mathrm{sgn}(\lambda)\frac{Q^2}{2} + \mathrm{sgn}(\mu)\frac{Q^4}{4} = h. \tag{15}$$

In the following section, all the solutions of equation (15) will be expressed as combinations of Jacobi elliptic functions [14] with moduli functionally connected to the value of the Hamiltonian function. The new variable is considered as ascending in value (i.e. representing forward-in-time processes of its dynamical analogue).

3. Exact travelling wave solutions of the GNLS

Three families of travelling wave solutions will be presented in the present section, namely solitary wave solutions, periodic wave solutions and unbounded solutions. We proceed with the presentation of the aforementioned solutions as follows.

3.1. Solitary wave solutions

In order to derive bright solitary wave solutions we consider case 1. In the new coordinate system (Q, P) the elliptic points are located at $(Q, P) = (\pm 1, 0)$ and the hyperbolic point at $(Q, P) = (0, 0)$. The respective values of the Hamiltonian are $h = -\frac{1}{4}$ and $h = 0$. Then, for $h = 0$, i.e. for the Hamiltonian value corresponding to the hyperbolic point, direct solution of equation (15) leads to the following solution, which has two branches, expressed in the form

$$Q_{\pm}^{(bs)}(\Sigma) = \pm\sqrt{2}\,\mathrm{sech}(\Sigma). \tag{16}$$

Shock wave solutions, or 'dark' solitary wave solutions (a term more proper if one refers to optical propagation), can be obtained upon considering case 2. In this case, there is an elliptic fixed point and two hyperbolic ones placed at $(Q, P) = (0, 0)$ and $(Q, P) = (\pm 1, 0)$, respectively. The respective values of the Hamiltonian are $h = 0$ and $h = \frac{1}{4}$. Then, for $h = \frac{1}{4}$, i.e. for the Hamiltonian value corresponding to the hyperbolic points, equation (13) leads to the following solution, having two branches, expressed as

$$Q_{\pm}^{(ds)}(\Sigma) = \pm\tanh(\Sigma/\sqrt{2}). \tag{17}$$

Note that the $(+)$ sign in equations (16) and (17), i.e. when $F > 0$, corresponds to the conventional form of the bright and dark solitary waves, respectively. On the other hand, the $(-)$ sign in equation (16), in the case $F < 0$, corresponds to a 'rarefaction' solitary wave (in the nomenclature of [12]) while the $(-)$ sign in equation (17) corresponds to a kink-like dark solitary wave.

3.2. Periodic wave solutions

In order to derive periodic wave solutions we consider, at first, case 1. When $-\frac{1}{4} \leqslant h < 0$, (sub-case 11) we obtain families of solutions with two branches having the form

$$Q_{\pm}^{(11)}(\Sigma) = \pm\left(\frac{2}{2-m_{11}}\right)^{1/2} \mathrm{d}n\,(\Sigma(2m_{11}-1)^{-1/2}, m_{11}) \tag{18}$$

where m_{11} is the elliptic modulus. The corresponding interval of the Hamiltonian values with respect to the modulus m_{11} can be found to be

$$-\frac{1}{4} < H = h(m_{11}) = -\frac{1-m_{11}}{(2-m_{11})^2} < 0 \qquad m_{11} \in (0,1). \tag{19}$$

On the other hand, when $h > 0$ (sub-case 12), we obtain another family of solutions which have the form

$$Q_{\pm}^{(12)}(\Sigma) = \pm\left(\frac{2m_{12}}{2m_{12}-1}\right)^{1/2} cn(\Sigma(2m_{12}-1)^{-1/2}, m_{12}) \tag{20}$$

where m_{12} is the respective elliptic modulus. The corresponding values of the Hamiltonian function are given by

$$\infty > H = h(m_{12}) = \frac{m_{12}(1-m_{12})}{(2m_{12}-1)^2} > 0 \qquad m_{12} \in (\tfrac{1}{2}, 1). \tag{21}$$

Comparing the values of the Hamiltonian given by equations (19) and (21), we observe that in the limit as m_{11} or $m_{12} \to 1$, the Hamiltonian becomes $H(m_{11} = m_{12} = 1) = 0$ and the period of the periodic waves given by equations (18) and (20) tends to infinity. In this case, both solutions, equations (18) and (20), converge to the asymptotic solutions given by equation (16), i.e. to the bright solitary wave solutions.

Case 2 is now under consideration. When $0 < h < \frac{1}{4}$, there are three families of solutions, as we will see, depending on the initial conditions. One family (sub-case 21) corresponds to the case where $|Q| \leqslant 1$. The respective solution represents a nonlinear periodic wave of the form

$$Q^{(21)}(\Sigma) = \left(\frac{2m_{21}}{1+m_{21}}\right)^{1/2} sn(\Sigma(1+m_{21})^{-1/2}, m_{21}). \tag{22}$$

The respective Hamiltonian value, h, expressed as a function of the modulus m_{21}, is given by the following inequality:

$$0 < H = h(m_{21}) = \frac{m_{21}}{(1+m_{21})^2} < \frac{1}{4} \qquad m_{21} \in (0,1). \tag{23}$$

Note that in the limit $m_{21} \to 1$ and when h goes to $\frac{1}{4}$ from below, the period of the aforementioned nonlinear periodic waves, equation (22), tends to infinity. As in the case of the bright solitary wave, it is observed that at this infinite period limit, the dark solitary wave (17) is born.

Case 4 is finally considered. The Hamiltonian value is solely non-negative in this case and all the respective solutions correspond to periodic waves. After some algebra, one can readily show that there exists a single family of solutions of the form

$$Q_{\pm}^{(4)}(\Sigma) = \left[\frac{2m_4(1-m_4)}{1-2m_4}\right]^{1/2} s\,\mathrm{d}(\Sigma(1-2m_4)^{-1/2}, m_4) \tag{24}$$

where the Hamiltonian value, as a function of the modulus m_4 of the elliptic function, is given by

$$0 < H = h(m_4) = \frac{m_4(1-m_4)}{(1-2m_4)^2} < \infty \qquad m_4 \in (0, \tfrac{1}{2}). \tag{25}$$

Note that for small values of the Hamiltonian (i.e. $m_4 \approx 0$), the solutions given by equation (24) behave like $\sin(\Sigma)$ as expected, that is, the modes exhibit a harmonic behaviour for small values of h.

3.3. Unbounded solutions

We consider first case 2. When $0 < h < \frac{1}{4}$, there exist two other families of solutions, when $-1-\sqrt{2} \leqslant Q < -1$, and $1 < Q \leqslant 1+\sqrt{2}$ (sub-cases $22^{\pm}$). They are of the form

$$Q_{\pm}^{(22)}(\Sigma) = \pm\left(\frac{2}{1+m_{22}}\right)^{1/2} ns(\Sigma(1+m_{22})^{-1/2}, m_{22}) \tag{26}$$

where m_{22} is the new elliptic modulus. The Hamiltonian value, h, is in the same interval as in sub-case 21 (see equation (23)) and, as a function of the modulus m_{22}, is given by

$$0 < H = h(m_{22}) = \frac{m_{22}}{(1+m_{22})^2} < \frac{1}{4} \qquad m_{22} \in (0,1). \tag{27}$$

In the same case (2), when $h > \frac{1}{4}$, two other families of nonlinear unbounded modes exist (sub-cases $24^{\pm}$). Their form is found to be

$$Q_{\pm}^{(24)}(\Sigma) = \pm\left(\frac{1}{2m_{24}-1}\right)^{1/2} sc(\Sigma(2(2m_{24}-1))^{-1/2}, m_{24})\,\mathrm{d}n\,(\Sigma(2(2m_{24}-1))^{-1/2}, m_{24}). \tag{28}$$

The Hamiltonian values, on the other hand, are in the interval

$$\infty > H = h(m_{24}) = \frac{1}{4(2m_{24}-1)^2} > \frac{1}{4} \qquad m_{24} \in (\tfrac{1}{2}, 1). \tag{29}$$

Note that in the limit $m_{24} \to 1$ (h goes to $\frac{1}{4}$), inspection of equation (28) shows that this family of solutions converge to the dark solitary wave solutions given by equation (17).

Finally, in case 2, for negative Hamiltonian values, $h < 0$, there are two additional families of solutions (sub-cases $23^{\pm}$). Their behaviour is similar to that of those in sub-cases $22^{\pm}$, differing only in their functional form, that is

$$Q_{\pm}^{(23)}(\Sigma) = \pm\left(\frac{2}{1-2m_{23}}\right)^{1/2} \mathrm{d}s\,(\Sigma(1-2m_{23})^{-1/2}, m_{23}). \tag{30}$$

The Hamiltonian H, on the other hand, expressed as a function of the modulus m_{23}, is given by

$$-\infty < H = h(m_{23}) = -\frac{m_{23}(1-m_{23})}{(1-2m_{23})^2} < 0 \qquad m_{23} \in (0, \tfrac{1}{2}). \tag{31}$$

Note that in the limit $m_{23}, m_{22} \to 0$, the Hamiltonian becomes $h(m_{23} = m_{22} = 0) = 0$ and inspection of equations (26) and (30) shows that both families of unbounded modes converge, as expected, to the following limiting modes:

$$Q_{\pm}^{(2t)}(\Sigma) = \pm\sqrt{2}csc(\Sigma). \tag{32}$$

On the other hand, in the limit m_{22}, $m_{24} \to 1$, the Hamiltonian value goes to $\frac{1}{4}$ too. Inspection of equations (26) and (28) shows that the family which corresponds to the former converge to modes given by

$$Q_{\pm}^{(2s)}(\Sigma) = \pm \coth(\Sigma/\sqrt{2}) \tag{33}$$

while the respective family of the latter equation converges to the dark solitary wave solutions given by equation (17).

We consider now case 3. The sole hyperbolic point in this case is placed at $(Q, P) = (0, 0)$. It is readily evident from equation (15) that unbounded solutions exist for all values of the Hamiltonian $h \in (-\infty, +\infty)$. Specifically, for the initial condition $Q(\Sigma = 0) = 0$, one can obtain the following families of solutions (sub-cases $31^{\pm}$):

$$Q_{\pm}^{(31)}(\Sigma) = \pm(1 - 2m_{31})^{-1/2} \frac{1 - cn(\Sigma(2(1 - 2m_{31}))^{-1/2}, m_{31})}{sn(\Sigma(2(1 - 2m_{31}))^{-1/2}, m_{31})} \tag{34}$$

with the Hamiltonian value in the following interval

$$\frac{1}{4} < H = h(m_{31}) = \frac{1}{4(1 - 2m_{31})^2} < \infty \qquad m_{31} \in (0, \tfrac{1}{2}). \tag{35}$$

For $0 < h < \frac{1}{4}$, and for the initial condition $Q(\Sigma = 0) = 0$, one obtains the following families of branches (sub-regions $32^{\pm}$, respectively adjacent to sub-regions $31^{\pm}$):

$$Q_{\pm}^{(32)}(\Sigma) = \pm \left(\frac{2(l - m_{32})}{2 - m_{32}} \right)^{1/2} sc(\Sigma(2 - m_{32})^{1/2}, m_{32}) \tag{36}$$

where the modulus m_{32} of the elliptic function involved and the Hamiltonian value are related through the following expression:

$$\frac{1}{4} > H = h(m_{32}) = \frac{1 - m_{32}}{2(2 - m_{32})^2} > 0 \qquad m_{32} \in (0, 1). \tag{37}$$

Note that as $h \to \frac{1}{4}(m_{31}, m_{32} \to 0)$ both expressions (34) and (36) converge to the modes given by

$$Q_{\pm}^{(0)}(\Sigma) = \pm \tan(\Sigma/\sqrt{2}). \tag{38}$$

Note that the solution (38) can be directly obtained via equation (15) by setting $h = \frac{1}{4}$.

Finally, in case 3, for $h < 0$, the following two branches of solutions can be obtained:

$$Q_{\pm}^{(33)}(\Sigma) = \pm \left(\frac{2(1 - m_{33})}{2m_{33} - 1} \right)^{1/2} nc(\Sigma(2m_{33} - 1)^{1/2}, m_{33}) \tag{39}$$

for the initial condition

$$Q(\Sigma = 0) = \pm \left(\frac{2(1 - m_{33})}{2m_{33} - 1} \right)^{1/2}.$$

In this case, the Hamiltonian value, h, expressed as a function of the modulus m_{33}, is given by

$$-\infty < H = h(m_{33}) = -\frac{m_{33}(1 - m_{33})}{(2m_{33} - 1)^2} < 0 \qquad m_{33} \in (\tfrac{1}{2}, 1). \tag{40}$$

In the limiting case $h \to 0^-(m_{33} \to 1^-)$ the solutions in equation (38) converge to the modes $Q_{\pm}^{(1)}(\Sigma) = \pm(2\varepsilon)^{1/2} \cosh(\Sigma)$, where $\varepsilon = 1 - m_{33} \simeq 0$. On the other hand, when $h \to 0^+(m_{32} \to 1^-)$ the solutions in equation (35) converge to the waves $Q_{\pm}^{(1)}(\Sigma) = \pm(2\varepsilon)^{1/2} \sinh(\Sigma)$, where $\varepsilon = 1 - m_{32} \simeq 0$. From the above discussion it is readily seen that in the limiting cases $h \to 0^+$, or $h \to 0^-$ the solutions (36) and (39) do

not converge to a *sole* asymptotic mode. Nevertheless, at $h = 0$ there exists an *isolated* solution that differs from the aforementioned asymptotic ones as $h \to 0^{\pm}$. This solution, which can be directly obtained from equation (15) by setting $h = 0$, is given by

$$Q_{\pm}^{(1)}(\Sigma) = \frac{Q_0}{\cosh(\Sigma) \pm \mathrm{sign}(Q_0)(1 + Q_0^2/2)^{1/2} \sinh(\Sigma)} \tag{41}$$

and corresponds to the initial condition $Q(\Sigma = 0) = \pm Q_0$ in either case.

4. Dynamics associated with the travelling wave solutions

It is convenient to represent now the solutions obtained in the previous section in a unified form, directly connected to the four cases of section 2. This can be easily done by considering the dynamics associated with these cases separately and illustrating the correspondence between the phase plane curves and the derived solutions by means of certain figures. As will be seen, this unification of the results will lead to some additional features of the travelling wave solutions of the GNLS. In this way, we proceed with the presentation of the above-mentioned cases as follows.

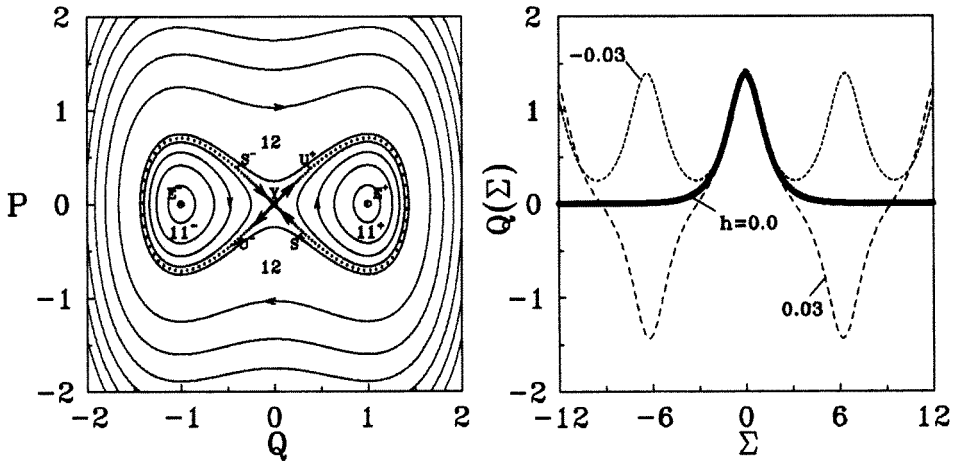

Figure 1. Case 1 ($\lambda < 0, \mu > 0$): phase plane curves for various normalized Hamiltonian values and $Q(\Sigma)$ diagrams. Sub-regions: $(11^{\pm}) -\frac{1}{4} < h \leqslant 0$, (12) $0 < h$; all bounded modes. The solitary wave solution corresponds to the figure-eight separatrix and the full curve in the respective diagrams. The arrows correspond to an increasing travelling wave coordinate Σ.

Case 1. In the phase plane diagram of figure 1 various phase curves which correspond to case 1 are shown, together with the hyperbolic fixed point Y and the pair of elliptic fixed points E^- and E^+. Four branches correspond to the hyperbolic point Y: two (U^+ and U^-) are outgoing in opposite directions. These are the (well known in dynamics) unstable branches. The other two branches (S^- and S^+) are ingoing and they represent the so-called stable branches. The branches U^+ and S^+ coincide, because the system is integrable; they form a separatrix (the thickly dotted line surrounding the point E^+). In the same way the coinciding branches U^- and S^- form a separatrix too. These separatrices correspond to the asymptotic bright solitary wave solutions, equation (16). As expected from the theory of dynamical systems, the separatrices separate regions of qualitatively different motions in the phase plane, namely the regions 11^+, 11^- and 12.

The phase curves in the regions 11^- and 11^+ surround the elliptic points E^- and E^+, respectively, for several values of the Hamiltonian in the interval $-\frac{1}{4} < h < 0$. These phase curves correspond to periodic solutions, equation (18), of different period. For the value of h being infinitesimally close to $\frac{1}{4}$ ($m_{11} \to 0^-$), that is, in the immediate vicinity of the elliptic fixed point, the period is finite ($= 2\pi$), though the corresponding amplitude is infinitesimally small. The associated wave solutions describe an almost linear wave, or in other words a continuous wave (cw) background solution exists for the original GNLS problem. As h increases, the elliptic modulus m_{11} increases also and the nonlinear character emerges: increasing amplitude is accompanied by increasing period. This period tends to infinity when $h \to 0^-(m_{11} \to 1^-)$, and thus the asymptotic solution (bright solitary wave) is obtained at $h = 0$.

The phase curves in region 12 ($h > 0$), on the other hand, surround both separatrices. Several periodic solutions of the type which equation (20) provides are shown. As h increases (m_{12} decreases) the period decreases and in the limit $h \to \infty$ the period approaches the value 2π. Oppositely, when $h \to 0^+(m_{12} \to 1^+)$, the period tends to infinity and the asymptotic solitary wave solution is obtained. In the vicinity of the latter, the period of the nonlinear waves of region 12 is twice the period of the corresponding ones (same value of the respective moduli) of region 11, a result consistent with the nonlinear pendulum picture of a nonlinear oscillator.

It should be noted that the periodic character of the nonlinear waves in regions 11 and 12 and the discontinuity in the periodicity caused by crossing the separatrix is clear in the $Q(\Sigma)$ diagrams in figure 1: two cases are shown for $h = 0.03$ (large broken curve) and $h = -0.03$ (fine broken curve). The thick full curve represents the asymptotic bright solitary wave solution.

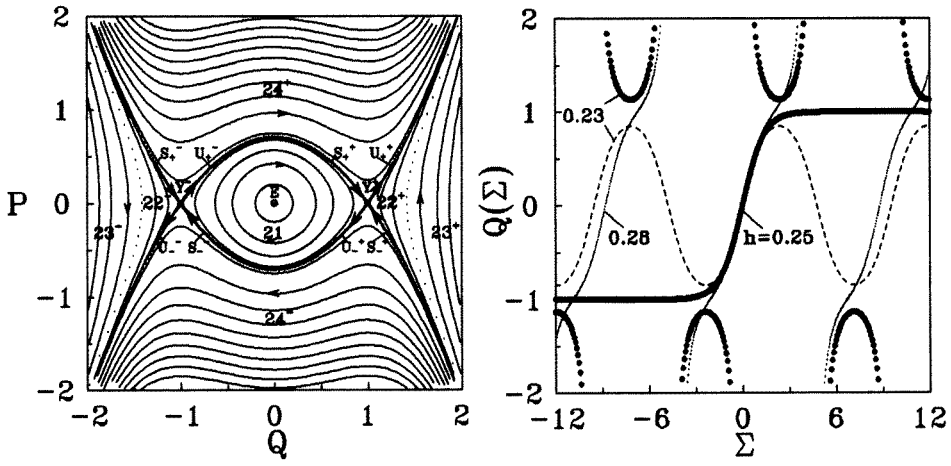

Figure 2. Case 2 ($\lambda > 0, \mu < 0$): phase plane curves for various normalized Hamiltonian values and $Q(\Sigma)$ diagrams. Sub-regions: (21) $0 < h \leqslant \frac{1}{4}$, bounded modes; ($22^{\pm}$) $0 < h \leqslant \frac{1}{4}$, unbounded modes; ($23^{\pm}$) $h \leqslant 0$, unbounded modes; ($24^{\pm}$) $\frac{1}{4} < h$, unbounded modes. The separatrix branches between the sub-regions 21 and $24^{\pm}$ correspond to regular dark solitary wave solutions, while the ones between the sub-regions $24^{\pm}$ and $22^{\pm}$ correspond to 'spiky' (unbounded at $\Sigma = 0$) wave forms. The full curve in the $Q(\Sigma)$ diagram represents the regular dark solitary wave solutions, while the spiky one (not shown) has the same $\Sigma = \pm 1$ asymptotic lines and $Q(\Sigma \to 0^{\pm}) \to \pm\infty$. The arrows correspond to an increasing travelling wave coordinate Σ.

Case 2. In figure 2 the phase diagram associated with case 2 is shown, together with the elliptic fixed point E ($h = 0$) at $(Q, P) = (0, 0)$ and the hyperbolic ones, Y^- and $Y^+(h = \frac{1}{4})$, at $(Q, P) = (\pm 1, 0)$. As far as the periodic wave solutions associated with this case are concerned, it is evident that they are represented as phase curves surrounding the elliptic fixed point E. One such wave solution, corresponding to the expression in equation (22), is shown for $h = 0.23$ (broken curve) in the $Q(\Sigma)$ diagram in figure 2. Note that for each initial point ($-1 < Q_0 < 1, P_0 = 0$) there corresponds a value of h in the interval $0 < h < \frac{1}{4}$. At the value $h = 0$, we have $Q = 0$ and $m_{21} = 0$. In this case the system is at rest. For a small variation of the value of $h = 0$ the periodic nonlinear waves (22) are born whose period increases as $h \to \frac{1}{4}$.

Let us consider now the unbounded wave solutions associated with case 2. At first, as far as the solutions given by equation (26) are concerned (sub-case 22), it is seen that they represent unbounded modes of finite 'period' (multiplier of Σ). The latter increases as m_{22} (or h) increases and tends to infinity as $m_{22} \to 1 (h \to \frac{1}{4})$. This 'period' has basically the meaning of a transition time, since the modes exhibit an explosive nature in a finite Σ-interval of the order of this 'period', as is evident from the $Q(\Sigma)$ diagrams of figure 2 (densely and thickly dotted curves for $h = 0.23$). Nevertheless, if other physical factors, not incorporated in the model in hand (a low level of dissipation, for example) come into play, this explosive nature can merely be modified to become a spiky behaviour. In such a case the separated explosive branches will communicate through sharp, almost vertical, transitions.

The family of solutions appearing in equation (28), which represent nonlinear unbounded modes as well, is the product of two Jacobi functions of the same period. Thus, $Q_{\pm}^{(24)}(\Sigma)$ has a finite 'period', which is equal to half the period of these functions. In the $Q(\Sigma)$ diagram in figure 2 one such solution is shown for $h = 0.28$ (finely and densely dotted curves). Several phase curves are also shown whose finite 'period' decreases as h increases. The unbounded modes for this interval of Hamiltonian values exhibit a compression–decompression behaviour. They differ, however, from those of sub-case 22 (equation (26)) since the latter do not pass through the value $Q = 0$, while the former do. On a similar basis, extraneous factors may cause bridging at the two (positive and negative) branches leading finally to a spiky behaviour twice as frequent as the one for sub-case 22.

As was shown in the previous section, the nature of the unbounded wave solutions in the regions $23^{\pm}$ (equation (30)) is identical to that of the adjacent regions $22^{\pm}$ (see figure 2). Several phase curves in regions $23^{\pm}$ are shown in the phase diagram in figure 2. They represent modes whose finite 'period' increases as $h \to 0$ from negative values. As far as the limiting solutions given by equation (32) are concerned, they correspond to the sparsely dotted curves in the phase diagram of figure 2. Of course, these limiting solutions are not classified as asymptotic ones, since they exhibit a finite 'period'. However, the limiting modes described by equation (33), although they are unbounded ones, can also be classified as solitary waves. This is true because (like those of equation (17)) they lead to travelling wave solutions to the original GNLS problem and exhibit a localized (in Σ) transition from the asymptotic state -1 (in the limit $\Sigma \to -\infty$) to the asymptotic state $+1$ (in the limit $\Sigma \to +\infty$) (see for example [15]). Moreover, their period is infinite. They may be characterized as explosive or implosive modes acting on a 'quiescent' background ($Q \approx \pm 1$) within a narrow interval close to $\Sigma = 0$. If extraneous factors are permitted to act, the two quiescent states can then be bridged through a spiky behaviour during their transit through $\Sigma = 0$. That is, in such a case, the 'shock wave' nature is preserved, though through a rather spiky transition instead of a smooth transition as compared to those described by equation (17).

Taking into account the previous discussion, let us now take a closer look at figure 2. For the sake of clarity, only the asymptotic solutions that correspond to the regular dark solitary wave are shown (thick full curve) in the $Q(\Sigma)$ diagram in this figure. The phase curves which correspond to the hyperbolic fixed points (equations (17) and (33)) form the separatrices (densely dotted curves in the phase diagram of figure 2). The branches U_-^+, S_+^+ and U_+^-, S_-^-, which separate region 21 from regions $24^\pm$ (upper and lower), coincide with the dark solitary wave solutions (equation (17)) $Q_\pm^{(ds)}$, respectively. The remaining branches separate regions $24^\pm$ from regions $22^\pm$. The outgoing and ingoing curves, U_+^+ and S_-^+, respectively (from and towards the hyperbolic point Y^+), correspond to the $Q_+^{(2s)}$ solution of equation (33). Similarly the branches S_+^- and U_-^- correspond to the $Q_-^{(2s)}$ solution of the same equation representing solitary modes of similar nature as we already have pointed out. It is also worth mentioning that for $h = 0$ one gets both the elliptic fixed point, E $[(Q, P) = (0, 0)]$ as well as the aforementioned non-asymptotic limiting phase curves (sparsely dotted curves, equation (32)) which correspond to initial conditions $(Q_0, P_0) = (0, \pm\sqrt{2})$. Since these curves do not represent separatrices, one can go from one region to the other (by continuously varying the value of h from negative to positive values, or vice versa) without affecting the character of the modes involved.

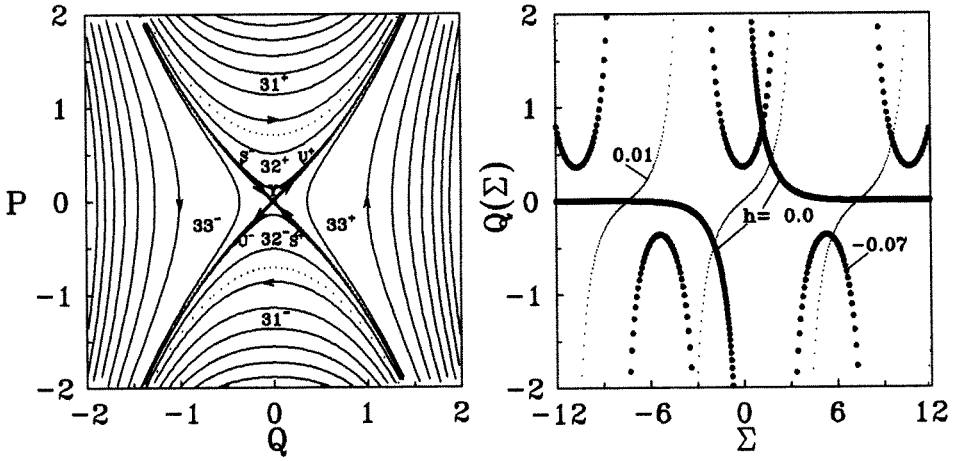

Figure 3. Case 3 ($\lambda < 0, \mu < 0$): phase plane curves for various normalized Hamiltonian values and $Q(\Sigma)$ diagrams. Sub-regions: $(31^\pm)\ \frac{1}{4} < h$, $(32^\pm)\ 0 < h \leqslant \frac{1}{4}$, $(33^\pm)\ h \leqslant 0$; all unbounded modes. The separatrices correspond to an isolated 'spiky' solitary mode for $h = 0$. This mode is shown by the thick curve in the $Q(\Sigma)$ diagram. The arrows correspond to an increasing travelling wave coordinate Σ.

Case 3. In figure 3, the phase diagram associated with case 3 is presented. As was shown in the previous section, the modes of either sub-cases $31^\pm$ or sub-cases $32^\pm$ are unbounded and exhibit an explosive–implosive character in a finite Σ-interval. Several phase curves of these sub-cases appear in the phase diagram of figure 3. Additionally, in the $Q(\Sigma)$ diagram of figure 3, these modes are presented, for $h = 0.01$, by the thinly dotted curves. As we have already pointed out in case 2, extraneous factors may cause the conversion of these seemingly unnatural modes into a spiky excitation through bridging maxima with minima.

As far as the unbounded solutions in equation (39) are concerned (corresponding to the two symmetric sub-regions $33^\pm$), they are presented in the $Q(\Sigma)$ diagram of figure 3

by several phase curves as well. In the $Q(\Sigma)$ diagram a single case for $h = -0.07$ is represented by thickly dotted curves. These modes, as in case 2, exhibit a compression–decompression behaviour in a finite Σ-interval, over a finite Q-background (Q never goes to zero) and can be bridged towards a spiky succession of compressions and decompressions through almost vertical transitions, if extraneous factors can come into play.

The limiting solutions (for $m_{31}, m_{32} \to 0$) appearing in equation (38) are also presented in the phase diagram of the same figure and are denoted by the two symmetric, sparsely dotted curves. These modes do not represent asymptotic solutions; they are simply transitional modes that conform to the continuity requirement of equations (34) and (36). On the other hand, the solutions given by equation (41) do represent asymptotic solutions (as discussed in the previous section) and thus they are solitary waves. This is true because they correspond to travelling waves in the original GNLS problem and their transition from the asymptotic state 0 (in the limit $\Sigma \to -\infty$) to the same asymptotic state 0 (in the limit $\Sigma \to +\infty$) is essentially localized in Σ. Moreover, we note that these waves are of infinite period.

In figure 3 these solitary modes have the form of the separatrices that separate subregions $33^{\pm}$ from $32^{\pm}$. In the $Q(\Sigma)$ diagram (thick full curve) their seemingly unnatural character can rather be described as a sudden (i.e. it takes place in a finite Σ-interval) explosion or implosion emerging from the quiescent state $Q(\Sigma) = 0$. Bridging maxima with minima will eventually lead to a behaviour characterized by a sudden single spike. The respective curves in the phase diagram in figure 3 consist of two pairs of branches, namely the S^-, U^+ and S^+, U^- pairs. The stable (S) branches are ingoing towards the hyperbolic point Y, while the unstable ones (U) are outgoing. These branches form the separatrices that separate the phase plane into sub-regions where the modes are qualitatively different. Their asymptotic character is in accordance with the solitary nature of the modes they represent.

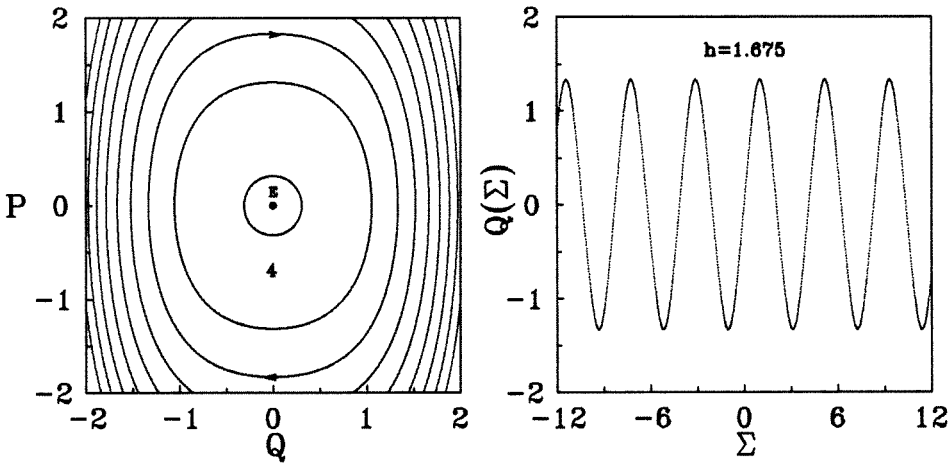

Figure 4. Case 4 ($\lambda > 0, \mu > 0$): phase plane curves for various normalized Hamiltonian values and $Q(\Sigma)$ diagrams for the sole region (4): $0 \leqslant h$. All modes correspond to bounded periodic waves. The arrows correspond to an increasing travelling wave coordinate Σ.

Case 4. In the phase plane diagram of figure 4 several phase curves which correspond to case 4 are shown, together with the sole elliptic fixed point E. As is readily seen, these curves represent periodic orbits (in the mechanical sense); they surround the elliptic point and correspond to periodic wave solutions (equation (24)) of the original GNLS equation.

A single periodic wave for $h = 1.675$ is also shown in the respective $Q(\Sigma)$ diagram.

5. Discussion and conclusions

In the present paper the class of the exact travelling wave solutions of the GNLS equation has been comprehensively derived and thoroughly studied. The obtained results are applicable to the problem of femtosecond pulse propagation in nonlinear optical fibres. The method of analysis adopted, which is based on analysing the problem in hand in the framework of the Hamiltonian dynamics, is capable of treating a whole class of nonlinear travelling wave modes. This class of solutions incorporates bright and dark solitary waves, periodic waves, unbounded solutions and other solitary modes as asymptotic limits of the periodic or unbounded modes derived and analysed in this work.

Using the travelling mode type of solution with nonlinear shifts to the carrier frequency, wave number and group velocity, the GNLS was reduced to a second-order ODE. This ODE resembles the one describing the dynamics of the unforced and undamped Duffing oscillator and its coefficients depend on the fibre properties. Thus, the study of the GNLS is reduced to the study of an integrable dynamical system. By completely analysing the aforementioned ODE, several conclusions concerning the problem under consideration were reached. Additionally, important remarks of far more general interest for physical systems obeying the generalized Duffing Hamiltonian (or even for systems with Hamiltonian behaviour in general) were also made. In the following, both special conclusions and general remarks are summarized.

5.1. General remarks

(1) Each of the derived exact solutions represents a two-parameter family of solutions, in the sense that it corresponds to a specific value h of the Hamiltonian function (equation (15)) and can be expressed in terms of the parameter λ (equation (7)). This can be easily seen by using the following example: Consider the dark solitary wave solution (case 2) corresponding to the value $h = \frac{1}{4}$. Then, using the expression for the envelope function, equation (17), together with equations (2)–(4) and (8), the dark solitary wave solution of the original GNLS problem can be expressed in terms of the parameter λ and the coefficients α, β, γ of the GNLS as follows:

$$q(t,x) = \pm\left(\frac{\lambda\alpha}{3\beta+2\gamma}\right)^{1/2}\tanh\left[\left(\frac{\lambda}{2}\right)^{1/2}(t-\Lambda x-\sigma_0)\right]\exp[\mathrm{i}(\kappa x-\Omega t-\theta_0)]. \tag{42}$$

In addition, in order to obtain a specific type of solution, the validity of several conditions is also required. For example, as far as the case of the dark solitary wave solution is concerned, the free parameter λ must be positive and the parameter μ must be negative (necessary conditions for case 2). Finally, the initial amplitude corresponding to the solution (42) must be given by

$$q(t,0) = \pm\left(\frac{\lambda\alpha}{3\beta+2\gamma}\right)^{1/2}\tanh\left(\left(\frac{\lambda}{2}\right)^{1/2}(t-\sigma_0)\right)\exp[-\mathrm{i}(\Omega t+\theta_0)] \tag{43}$$

and the initial phase must be fixed according to equations (9)–(11).

(2) All the *asymptotic* solutions are characterized by infinitely long period. They are basically all solitary modes and correspond to separatrices on the phase plane (or on the Poincaré plane of sections for a system of two degrees of freedom). The separatrices separate regions of the phase plane characterized by a qualitatively different type of behaviour. They

separate regions where the behaviour is bounded and periodic from regions where the motion is unbounded, as in case 2 (figure 2). They may separate regions of periodic behaviour but with different localizations and periodicities, as in case 1 (figure 1). They may finally separate regions of unbounded non-periodic behaviour with different localization, as in case 3 (figure 3). However, there may exist solitary modes (in the sense of having infinite period and being localized) which are not necessarily asymptotic. We will encounter such a case in what follows.

(3) The unbounded wave solutions (encountered in cases 2 and 3) may seem to correspond to states that are not physically realizable (or, at least, not all). However, there has been no conclusive argument in the literature concerning the realizability of the unbounded modes (see, for instance, [16]). On the contrary, there has been some evidence for the possibility of their existence in other disciplines of applied physics where equations of the nonlinear Schrödinger family are the working model: to mention just one, phase transitions in systems far from equilibrium (see, for example, [17]). Therefore, we feel reluctant in totally rejecting these unbounded modes. After all, the notion 'unbounded' has a rather relative value in a realistic, bounded system where other mechanisms capable of cutting off a limitlessly growing mode (optical signal if one specializes in the problem in hand) may well have been ignored in the first place.

(3.1) For sub-cases 22 (or 23) and 24 if physical factors not incorporated in the model in hand (a low level of dissipation, for example) come into play, this explosive nature of the respective modes can merely be modified to become a spiky behaviour. Thus, in such a case the separated explosive branches will communicate through sharp, almost vertical, transitions. The difference between sub-case 22 (or 23) and 24 merely lies in the passing of the respective amplitude of the latter through zero in the ideal (no extraneous factors invoked) case.

(3.2) The separatrices that separate the sub-regions 22 and 24 correspond to asymptotic solutions. Although unbounded at $\Sigma = 0$, they can safely be characterized as solitary modes: they merely lead to travelling wave solutions to the original GNLS problem and exhibit a localized (in Σ) transition from the asymptotic state -1 (in the limit $\Sigma \to -\infty$) to the asymptotic state $+1$ (in the limit $\Sigma \to -\infty$). Moreover, their period is infinite. As far as their physical content is concerned, they are explosive or implosive modes acting on a 'quiescent' background ($Q \approx \pm 1$) within a narrow interval close to $\Sigma = 0$. If extraneous factors are permitted to act, the two quiescent states can then be bridged through a spiky behaviour during their transit through $\Sigma = 0$. Therefore, they can be characterized as 'spiky shock waves' in contrast to the regular ones that correspond to the separatrices between the sub-regions 21 and 24.

(3.3) In case 3 all the modes are unbounded and, as in case 2, they may lead to spiky modes as explained earlier. The separatrices that separate sub-regions 33 from sub-regions 32, on the other hand, correspond to the *isolated* solutions for the case $h = 0$. They cannot be considered as the common asymptotic limit of the respective families of modes as $h \to 0^{\pm}$, since such a limit does not exist besides the sole hyperbolic point they are passing through. The separatrices of case 3, therefore, are physically realizable only as isolated and not asymptotic modes. However, they are indeed solitary modes because they correspond to travelling modes in the original GNLS problem exhibiting a localized transition from the asymptotic state 0 (in the limit $\Sigma \to -\infty$) to the same asymptotic state 0 (in the limit $\Sigma \to +\infty$). If extraneous factors are invoked this transition will merely be reduced to a single spike. They may, therefore, be characterized as 'solitary spikes'.

(4) As far as the stability of the bounded solutions (cases 1, 2.1 and 4) is concerned, one may simultaneously apply an amplitude and phase modulation (i.e. perturbing the elliptic

function as well as its initial phase) on the solutions found and feed the result back into equation (1). This procedure is quite common in cases encountered in the literature, such as the study of the modulational instability of the original GNLS, equation (1), [18] and certain versions of it ($\alpha = \gamma = 0$) [19]. Fully examining the stability of the derived bounded solutions is beyond the scope of this work. However, it can be readily shown that in the simple case of a sole localized amplitude modulation, $\delta Q(\Sigma)$, the linearized equation that δQ obeys is

$$\frac{\mathrm{d}^2\delta Q}{\mathrm{d}\Sigma^2} + [\mathrm{sgn}(\lambda) + Q_0^2(\Sigma)\,\mathrm{sgn}(\mu)]\delta Q = 0 \tag{44}$$

where $Q_0(\Sigma)$ are the respective bounded travelling wave solutions. This is a Hill's-type equation, different for each sub-case which the solution Q_0 represents. It is well known [20] that there exist stability intervals associated with the Hill equation whose structure depends upon the value of the modulus, m, which enters into Q_0. Since the modulus m is directly related to the value of the Hamiltonian function, the stability question is closely connected to the value of the latter, and the functional form of Q_0, of course. A complete study of equation (44) is, by itself, a very interesting problem and a subject of future investigation.

5.2. Special conclusions

(1) The parameter which parametrizes the various families of nonlinear modes in their respective sub-cases is the normalized Hamiltonian value (equation (13)). This parameter is directly related to the initial conditions (F_0', F_0') of the pulse. On the other hand, the parameters that distinguish one case from another are λ and μ. The former is a free parameter, which determines the nonlinear shifts in wave number and velocity (see equations (10)–(11)), while the latter is a constant related to the coefficients of the GNLS (see equation (8)). The parameter λ is allowed to take both positive and negative values, while the sign of the parameter μ depends on the signs of the coefficients of the GNLS equation. However, in the particular problem of femtosecond pulse propagation in optical fibres, the parameters β and γ are always positive [5–10]. Thus, the sign of the parameter μ depends solely on the sign of the coefficient α, which is proportional to the third-order linear dispersion $\partial^3 k/\partial\omega^3$. For graded index fibres this parameter is always positive, and thus μ is negative. On the other hand, for quadruple-clad fibres, it can take both positive and negative values, depending on the operation wavelength ($\partial^3 k/\partial\omega^3 > 0$ for $\lambda \lesssim 1.45\ \mu$m and $\partial^3 k/\partial\omega^3 < 0$ for $\lambda \gtrsim 1.45\ \mu$m) [10].

(2) The bright or dark solitary wave formation is connected with the necessary conditions $\mu < 0$ (case 1) or $\mu > 0$ (case 2), respectively. According to the aforementioned discussion, it can readily be concluded that the possibility of bright (dark) solitary wave formation is predicted for $\partial^3 k/\partial\omega^3 < 0$ ($\partial^3 k/\partial\omega^3 > 0$). It is important to mention that there is no imposition concerning the value of the parameter s. This means that the expressions in equations (16)–(17) form families of solitary wave solutions, which can be supported in both the normal ($s = +1$) and the anomalous ($s = -1$) dispersion regimes. Notice that this result has been reported elsewhere [1, 9] and stands in the case of propagation at the so-called zero dispersion point (corresponding to zero GVD, or $s = 0$) as well [10].

(2.1) As far as the anomalous dispersion regime is concerned, the possibility of dark pulse propagation is in sharp contrast with the conventional form of the NLS, or versions of the GNLS arising for $\alpha = \gamma = 0$ [21, 22], where dark soliton (or solitary wave) solutions hold solely in the normal dispersion regime. It is also noted that since the derived dark solutions are exact solutions to a non-integrable system, i.e. equation (1), are in principle

different from either exact solutions of an integrable system [21], or perturbative solutions of a non-integrable system [22].

(2.2) An analogous result holds in the case of the normal dispersion regime as well, where the possibility of bright solitary wave propagation is predicted. In addition, it is worth noting that the derived bright solutions in equation (16) exhibit a constant phase, determined by equations (3) and (9)–(11). Thus, they are in principle different than other bright solutions (valid solely in the anomalous dispersion regime) of versions of the GNLS arising for $\alpha = \gamma = 0$ [23, 24], exhibiting an *a priori* assumed phase-modulation.

(3) For case 1, the minimum value of the normalized Hamiltonian value is $-\frac{1}{4}$. The bright solitary wave solution corresponds to $h = 0$ and all the respective mode solutions of the GNLS are bounded periodic nonlinear waves. On the other hand, in case 2 solutions exist for all values of h. Nevertheless, the allowable values of the Hamiltonian in order *bounded* modes to exist are $0 \leqslant h \leqslant \frac{1}{4}$ with a dark solitary wave solution corresponding to $h = \frac{1}{4}$. On the other hand, for cases 3 and 4, solutions exist for all the non-negative values of $H (H \geqslant 0)$. They are all unbounded, for case 3, while, for case 4, they are all bounded periodic waves.

(4) In the problem of femtosecond pulse propagation in optical fibres, an additional term of dissipative character may also be included in the RHS of equation (1). This so-called Raman term, which is of the form $\delta q \partial/\partial t[|q|^2]$, where δ is a real constant, describes the self-induced Raman effect [6–7], which gives rise to a frequency down-shift of bright solitons [6], or leads to a temporal self-shift of dark solitons [25]. The Raman term has not been included in equation (1) because conditions have been found for which it can be neglected [7] or compensated through various amplification schemes [26–28]. It should be noted that inclusion of the Raman term in the GNLS [18] would lead to a contribution of the form $+2\delta F^2 F'$ in equation (5). In such a case, the Hamiltonian structure which characterizes the family of the travelling wave solutions ceases to exist. In other words, the system of equations (5)–(6) cannot be made consistent any more via a set of consistency relations such as equations (7)–(8). Localized travelling wave solutions (exact) cannot be found if the Raman term is included. Nevertheless, the analysis presented in the present work is valid under the assumption that the normalized power of the envelope, defined as $P = F^2$, satisfies the following inequality:

$$\frac{2\delta}{|1 + \beta\Omega|} \ln\left(\frac{\mathrm{d}P}{\mathrm{d}\sigma}\right) \ll 1 \tag{45}$$

where Ω is given by equation (9). This condition for the envelope power is actually a requirement for minimization of the dissipative effect the Raman term may have on travelling wave propagation.

References

[1] Potasek M J and Tabor M 1991 *Phys. Lett.* **154A** 449
[2] Mihalache D, Torner L, Moldoveanu F, Panoiu N-C and Truta N 1993 *J. Phys. A: Math. Gen.* **26** L757
[3] Mihalache D, Panoiu N-C, Moldoveanu F and Baboiu D-M 1994 *J. Phys. A: Math. Gen.* **27** 6177
[4] Zheng W 1994 *J. Phys. A: Math. Gen.* **27** L931
[5] Kodama Y 1985 *J. Stat. Phys.* **39** 597
[6] Kodama Y and Hasegawa A 1987 *IEEE J. Quantum Electron.* **QE-23** 510
[7] Potasek M J 1989 *J. Appl. Phys.* **65** 941
[8] Frantzeskakis D J, Hizanidis K and Polymilis C 1995 *J. Opt. Soc. Am.* B **12** 687
[9] Potasek M J 1993 *IEEE J. Quantum Electron.* **QE-29** 281
[10] Frantzeskakis D J, Hizanidis K, Tombras G S and Belia I 1995 *IEEE J. Quantum Electron.* **QE-31** 183
[11] Ablowitz M J and Segur H 1981 *Solitons and the Inverse Scattering Transform* (Philadelphia, PA: SIAM)

[12] Infeld E and Rowlands G 1990 *Nonlinear Waves, Solitons and Chaos* (Cambridge: Cambridge University Press)
[13] Wiggins S 1990 *Introduction to Applied Nonlinear Dynamical Systems and Chaos* (New York: Springer)
[14] Abramowitz M and Stegun I A 1970 *Handbook of Mathematical Functions* (New York: Dover)
[15] Scott A C, Chu F Y F and McLaughlin D W 1973 *Proc. IEEE* **61** 1443
[16] Kaup D J, Reiman A and Bers A 1979 *Rev. Mod. Phys.* **51** 275
[17] Buttiker M and Thomas H 1978 Stability of nonuniform states in systems exhibiting continuous bifurcations *Solitons and Condensed Matter Physics* ed A R Bishop and T Schneider (New York: Springer)
[18] Potasek M J 1987 *Opt. Lett.* **12** 921
[19] Shukla P K and Rasmussen J J 1986 *Opt. Lett.* **11** 171
[20] Churchill R C, Pecelli G and Rod D L 1980 *Arch. Rat. Mech. and Anal.* **73** 313
[21] Vekslerchik V E 1991 *Phys. Lett.* **153A** 195
[22] Kivshar Yu S 1991 *Phys. Rev.* A **43** 1677
[23] Anderson D and Lisak M 1983 *Phys. Rev.* A **27** 1393
[24] Ohkuma K, Ichikawa Y H and Abe Y 1987 *Opt. Lett.* **12** 516
[25] Kivshar Yu S 1990 *Phys. Rev.* A **42** 1757
[26] Doran N J and Wood D 1988 *J. Opt. Soc. Am.* **5** 1301
[27] Kurokawa K and Nakazawa M 1991 *Appl. Phys. Lett.* **58** 2871
[28] Ding M and Kikuchi K 1992 *IEEE Photon. Technol. Lett.* **4** 497